# Stability of rock-armoured mild slopes

Jumelet, Daan; van Gent, Marcel R.A.; Hofland, Bas; Kuiper, Coen

**DOI**
10.1016/j.coastaleng.2023.104418

**Publication date**
2024

**Document Version**
Final published version

**Published in**
Coastal Engineering

**Citation (APA)**
Jumelet, D., van Gent, M. R. A., Hofland, B., & Kuiper, C. (2024). Stability of rock-armoured mild slopes. *Coastal Engineering*, *187*, Article 104418. https://doi.org/10.1016/j.coastaleng.2023.104418

Coastal Engineering 187 (2024) 104418

Contents lists available at ScienceDirect

Coastal Engineering

journal homepage: www.elsevier.com/locate/coastaleng

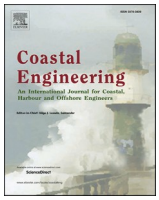

# Stability of rock-armoured mild slopes

Daan Jumelet [a], Marcel R.A. van Gent [b,c,*], Bas Hofland [c], Coen Kuiper [c,d]

[a] De Vries & van de Wiel, DEME, Amsterdam, the Netherlands
[b] Dept. Coastal Structures & Waves, Deltares, Delft, the Netherlands
[c] Dept. Hydraulic Engineering, Delft University of Technology, Delft, the Netherlands
[d] Witteveen+Bos, Deventer, the Netherlands

ARTICLE INFO

*Keywords:*
Coastal structures
Armour stability
Rock slopes
Mild slopes
Wave loading
Erosion
Damage characterisation
Slope protection
Physical model tests
Design guidelines

ABSTRACT

Physical model tests have been performed to study static stability of rock-armoured mild slopes. Current stability design formulae for steeper rock-armoured slopes focus on plunging and surging waves. Slopes of 1:6 and milder usually have more spilling breakers which decreases the load. Also, on mild slopes displaced rocks more often remain present in the wave attack zone, which increases the strength. These aspects lead to an overdesigned structure when existing formulae for steep rock-armoured slopes are used. The present wave flume tests were used to understand the processes and develop a design formula for rock-armoured mild slopes with an impermeable core. These tests were performed for statically stable rock-armoured slopes of 1:6 to 1:10. The tests confirmed that not all existing damage parameters are able to accurately describe the static stability on milder slopes. For mild slopes it is more accurate to describe the damage based on the eroded depth rather than on the eroded area or number of moved stones. In this study, a design formula and guidelines are provided for practicing engineers that design or evaluate the stability of mild rock-armoured slopes.

## 1. Introduction

Rock-armoured slopes are usually slopes steeper than 1:6 to minimize the slope length and the material volumes. Generally, steeper slopes require larger stone sizes in the armour layer, possibly larger stones in the filter layer, and potentially an additional filter layer compared to mild slopes (here defined as 1:6 or milder) with smaller armour material. Also, there are situations where natural foreshores are formed if the structure has a mild slope with low wave reflection characteristics. For example, the natural foreshores in front of dikes in the estuary Eastern & Western Scheldt in the Netherlands have slopes of 1:25 or gentler. In addition, the protection of pipeline and cable landings often requires rock armour layers with a mild slope. In case the natural foreshore erodes landwards, the foreshore slopes must be stabilized to prevent further erosion towards the dike. This can be achieved by applying mild slopes of the dike. Another example is when realizing a new bank protection, a mild slope can be chosen, whereby the required armour stone can be smaller, which in some cases is a solution if coarser stones are not locally available. In literature extensive information is available about static stable structures with a steep slope (*e.g.* Hudson, 1959; Van der Meer, 1988; Van Gent et al., 2003, 2019; Herrera et al., 2017; Etemad-Shahidi et al., 2020) or dynamic stable structures with mild slopes (*e.g.* Allan and Komar, 2004; Loman et al., 2010; Van Gent, 2010; Bayle et al., 2020, 2021). Research about statically stable rock-armoured mild slopes is scarce. The Rock Manual (2007) quantifies a statically stable structure roughly as a structure with a stability number $H_s/\Delta D_{n50} < 4$. A dynamically stable structure can be quantified with a stability number $H_s/\Delta D_{n50} > 6$. Statically stable structures are defined as structures for which no or limited damage is allowed during extreme conditions and dynamically stable structures are structures where profile development is accepted. These quantifications are based on research of steep structures, such as rubble mound breakwaters and on dynamically stable structures, such as gravel or cobble beaches.

Contrary to steep slopes, for mild slopes (defined here as $\cot\alpha \geq 6$) statically stable slopes can be obtained for stability numbers of $H_s/\Delta D_{n50} > 6$. Extrapolating design guidelines for steep statically stable structures or dynamically stable structure is not appropriate for statically stable mild slopes (further discussed in Section 2). To fill the gap in data, in this study physical model tests have been performed to describe the stability of rock-armoured statically stable mild slopes (presented in Section 3). This provides information to derive a dedicated design guideline for statically stable mild slopes (Section 4). Finally,

* Corresponding author. Dept. Coastal Structures & Waves, Deltares, Delft, the Netherlands.
*E-mail address:* m.r.a.vangent@tudelft.nl (M.R.A. van Gent).

https://doi.org/10.1016/j.coastaleng.2023.104418
Received 21 June 2023; Received in revised form 29 September 2023; Accepted 22 October 2023
Available online 27 October 2023

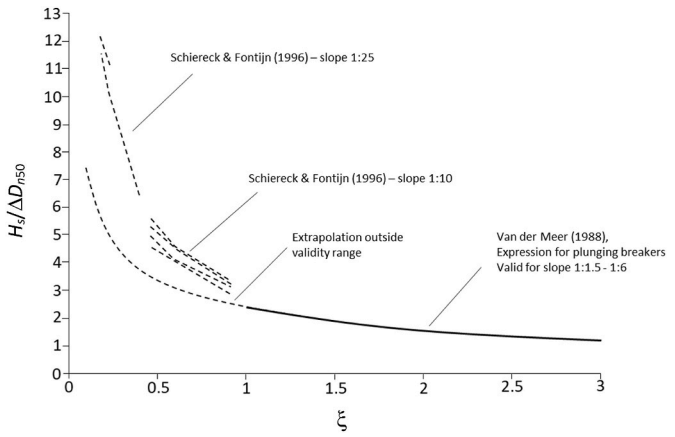


**Fig. 1.** Results of experiments carried out on a slope of 1:10 and 1:25 (Schiereck and Fontijn, 1996), where the vertical axis shows the stability number $H_s/\Delta D_{n50}$ and the horizontal axis shows the surf-similarity parameter based on the mean wave period.

conclusions and recommendations for future research are provided (Section 5).

## 2. Stability of rock-armoured slopes

### 2.1. Mild slopes

Mild slopes tests (1:10 and 1:25) by Sistermans (1993), Ye (1996), Schiereck et al. (1994) and Schiereck and Fontijn (1996) showed that for such mild rock-armoured slopes extrapolation of the stability formula by Van der Meer (1988) for rock-armoured slopes (with the majority of tests with slopes steeper than 1:4) provides conservative estimates of the required stone diameter (see also Fig. 1 by Schiereck and Fontijn, 1996).

Table 1 shows the slopes and ranges of the stability numbers in earlier mentioned tests. In the present study the focus is on mild slopes in the range of 1:6 to 1:10. This is milder than the steeper slopes used by Van der Meer (1988), and steeper than the range of the tests by Sistermans (1993) and Ye (1996).

Similar to tests by Thompson and Shuttler (1975) and Van der Meer (1988), here the focus is on rock-armoured slopes in relatively deep water with a horizontal bed and a high crest. Due to the deep water situation no wave breaking occurs on the foreshore. To estimate the stability of steep rock-armoured slopes in shallow water reference is made to Van Gent et al. (2003), Rock Manual (2007), Etemad-Shahidi et al. (2020) and Van der Meer (2021).

For steeper slope (*i.e.* 1:4 or steeper) wave breaking on the slope can be characterized by plunging or surging. In case the slope becomes more gentle a larger fraction of the waves can be characterized by spilling waves, while the fraction of plunging waves reduces for milder slopes. The jet-like wave loading on the slope as occurs for plunging waves, is not present for spilling waves. For spilling waves energy dissipation is more spread over the slope, see Fig. 2.

The spilling breakers result in wave loading and consequently damage over a larger part of the slope. On the contrary, plunging breakers lead to high wave loading and consequently damage at a specific point on the slope. This difference in wave breaking indicates that stability formula derived for plunging and surging waves on the slope (*e.g.* Van der Meer, 1988) should not be used for mild slopes without validation for such mild slopes.

Besides that the damage itself is affected by the slope, also the amount of allowable damage is affected by the slope angle. Many researchers used the eroded area $A_e$ in a cross-section by comparing the surface profiles before and after a test (Broderick, 1983, 1984). Criteria on the amount of allowable damage have been proposed based on the non-dimensional eroded area $S = A_e/D_{n50}^2$. Failure is often defined as the situation for which the filter layer underneath the armour layer is visible. This is more affected by the erosion depth (*i.e.* the reduction in thickness of the armour layer due to displaced stones) rather than the eroded area ($A_e$ or $S$), see for instance De Almeida et al. (2019). For milder slopes the damage is spread over a wider part of the slope than for steeper slopes. Thus, for the same eroded area, the erosion depth is generally less for milder slopes. Consequently, also the amount of allowable damage depends on the slope angle if the eroded area ($A_e$ or $S$) is used to characterize damage. Table 2 shows the damage criteria for a rock armour layer of two diameters thick as proposed in the Rock Manual (2007).

Although stability formulae for statically stable structures such as described in the Rock Manual (2007) can be applied to slopes between 1:1.5 and 1:6, lack of accurate design methods for mild slopes ($\cot\alpha \geq 6$) led to applying formulae for steep slopes also for mild slopes.

Wit (2015) discussed the relationship between allowable damage and the slope. Assuming that for each slope angle the damage remains between the same vertical reference points (*e.g.* one wave height above and below the still water level), the maximum allowable amount of damage can be calculated for slopes milder than those shown in Table 2 using a simple geometrical relation: $S_{mild} = S_{reference} \cdot (\sin\alpha_{reference}/\sin\alpha_{mild})$. If the allowable damage for a 1:4 slope is used as the reference, the allowable amount of damage for 1:6, 1:8 and 1:10 slopes would be respectively a factor 1.5, 2 and 2.5 higher than for a 1:4 slope. According to this first estimate, failure would respectively occur at $S = 25$, $S = 33$ and $S = 41$ for 1:6, 1:8 and 1:10 slopes (with $S = 17$ for a 1:4 slope as reference). Table 3 shows the values for start of damage and failure if a 1:4 slope with start of damage at $S = 3$ and failure at $S = 17$ is used as a reference.

Note that the assumption that for each slope angle the damage remains within the same vertical reference points, is an unvalidated assumption. Nevertheless, Table 3 illustrates that the damage criteria depend on the slope angle if the eroded area ($A_e$ or $S$) is used to characterize damage.

From aforementioned follows that the static stability formulations for steep slopes cannot be applied to static stability of mild slopes, neither to estimate the amount of damage, nor to derive a criterion for the amount of allowable damage at mild slopes. For these reasons, additional research into static stability of rock-armoured mild slopes is required.

**Table 1**
Tested mild slopes and ranges of the stability number in earlier studies.

| Author (year) | Seaward slope (cot α) | Stability number ($N_s = H_s/\Delta D_{n50}$) |
|---|---|---|
| Sistermans (1993) | 25 | 6–19 |
| Schiereck et al. (1994) | 25 | 4–13 |
| Ye (1996) | 10<br>25 | 3–6<br>6.5–12 |
| Schiereck and Fontijn (1996) | 10<br>25 | 3–5.5<br>6.5–12 |

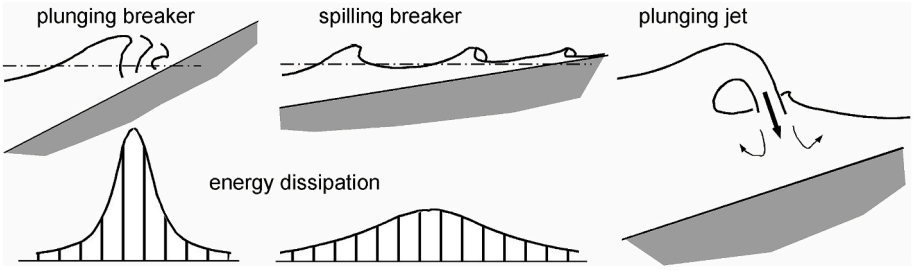


**Fig. 2.** Energy dissipation for spilling and plunging breakers with an example of a plunging jet phenomenon (Schiereck et al., 1994).

**Table 2**
Damage criteria for damage parameter $S = A_e/D_{n50}^2$ (Rock Manual, 2007).

| cot α | S (Start of damage) | S (Failure) |
|---|---|---|
| 1.5 | 2 | 8 |
| 2 | 2 | 8 |
| 3 | 2 | 12 |
| 4 | 3 | 17 |
| 6 | 3 | 17 |

**Table 3**
Damage criteria for damage parameter $S = A_e/D_{n50}^2$ using earlier criteria for 1:4 as reference.

| cot α | S (Start of damage) | S (Failure) |
|---|---|---|
| *1.5* | 1.3 | 7 |
| *2* | 1.6 | 9 |
| *3* | 2.3 | 13 |
| **4** | **3.0** | **17** |
| *6* | 4.4 | 25 |
| *8* | 5.9 | 33 |
| *10* | 7.3 | 41 |

### 2.2. Damage parameters

Section 2.1 describes that applying the non-dimensional damage parameter $S = A_e/D_{n50}^2$ (Broderick, 1983, 1984) has disadvantages. For steeper slopes other damage parameters have been discussed in for instance Melby and Kobayashi (1998), Hofland et al, (2011, 2014), Van Gent et al, (2019) and de Almeida et al, (2019). A number of damage parameters are discussed here before a selection is made for use in the analysis of the present test results.

The damage parameters described in this section can be divided into two-dimensional (2D) and three-dimensional (3D) damage parameters, shown in Fig. 3. The physical difference is that 2D-parameters are based on the damage from a width-averaged profile (Fig. 3a). A 3D-parameter (Fig. 3b) can be interpreted as a spatial moving average covering the entire slope based on a circle with a specific diameter.

The following damage parameters are discussed:

$$S = \frac{A_{e,w}}{D_{n50}^2} \tag{1}$$

where $A_e$ is the eroded area comparing the width-averaged initial profile with the width-averaged profile after wave attack (Broderick, 1983, 1984). This profile is width-averaged over the test section with width $w$. If more than one erosion area exists in the width-averaged profile, some authors only use the largest erosion area in this width-averaged profile, ignoring the erosion in the other erosion areas (*e.g.* Van der Meer, 1988), while in other studies (*e.g.* Van Gent and Wolters, 2015; Van Gent et al., 2019) the entire eroded area is considered as erosion, irrespective of the number ($n$) of erosion areas in a width-averaged profile:

$$S_{all} = \frac{A_{e1,w} + A_{e2,w} + \ldots + A_{en,w}}{D_{n50}^2} \tag{2}$$

$$E_{2D} = \frac{\max\left[(d_e)_w\right]}{D_{n50}} \tag{3}$$

The damage parameter $E_{2D}$ was introduced by Melby and Kobayashi (1998), where $d_e$, is the maximum slope-normal distance between the initial slope and the damaged slope in the tests, based on the width-averaged profile over the test section (see also De Almeida et al., 2019).

$$E_{3D} = \frac{\max\left[(d_e)_{m*D_{n50}}\right]_w}{D_{n50}} \tag{4}$$

where $d_e$ is the maximum depth of erosion perpendicular to the slope based on a moving average over a circular area of $m$ * $D_{n50}$ (Hofland et al., 2014) within the test section with width $w$. First, the erosion depth $d_e$ is determined for each position on the slope. Then, for each position on the slope, the values of $d_e$ are averaged over a circle of $m$ * $D_{n50}$ around that position. Thereafter, the maximum value obtained over the entire structure determines the value $E_{3D}$. If the averaging is applied over a circle with a diameter of 3 $D_{n50}$ (thus $m = 3$), then the notation is $E_{3D,3}$. A higher value of $m$ leads to an increase in the spatially moving circle, which is accompanied by a lower acceptable value for start of damage, intermediate damage and failure of the structure. Hereafter values $m = 1$, 3 and 5 are discussed.

These damage parameters are all profile based damage parameters. A damage parameter that is not based on the profile but on the number of displaced stones or units is:

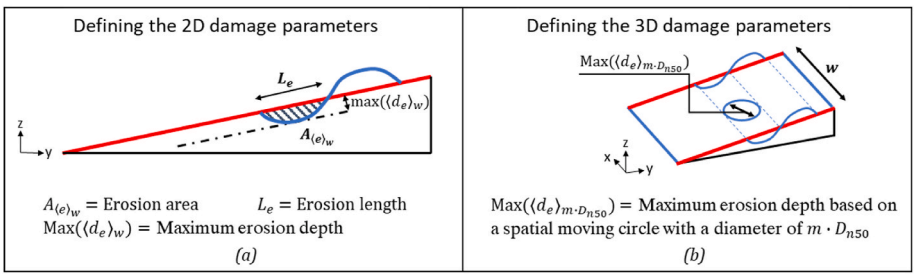


**Fig. 3.** (a) Schematization for 2D damage parameters $S$ and $E_{2D}$, (b) Schematization for 3D damage parameter $E_{3D,m}$; note that accretion can also (partly) occur below the erosion area (*e.g.* for steep slopes).

$$N_{od} = \frac{n_{tot} D_{n50}}{w} \quad (5)$$

where $n_{tot}$ is the number of displaced stones. The damage parameter $N_{od}$ (see also the Rock Manual, 2007) requires that all individual stone displacements are considered as damage. This method is less interesting for an efficient design method, as a displaced stone may contribute to the stability of the slope at another location. For large numbers of displaced stones, a difficulty in using this damage parameter is the measurement errors that are almost inevitable because stones that displace within the same color band (see also Fig. 5) cannot be clearly distinguished. Since mild slopes go together with relatively small stones and therefore a relatively large number of stones is present in the slope, $N_{od}$ has not been considered for mild slopes here.

#### 2.2.1. Evaluation of damage parameters

The damage parameter $S$ focuses on the largest erosion area in a width-averaged profile while $S_{all}$ considers all erosion areas in the width-averaged profile. Van Wijland (2020) provided evidence that for a 1:8 slope, on average the parameter $S$ does not include approximately 55 percent of the erosion on the slope compared to damage parameter $S_{all}$. Therefore, $S_{all}$ is preferred over $S$ to describe the amount of erosion of the armour layer. Hereafter, in this document $S$ refers to $S_{all}$ since the definition shown in Eq. (2) is preferred in this research.

The damage level $S$ does not show how erosion is distributed over the slope; erosion can take place over a relatively large length while a relatively small erosion depth occurs, but the same value for $S$ can be obtained for erosion that occurs over a relatively wide section in combination with a large erosion depth. Therefore, the damage parameter $S$ is less suitable to estimate whether the filter layer becomes exposed or not, especially for milder slopes where damage occurs over a wider section than for steeper slopes.

Because the damage parameters $S$ and $E_{2D}$ are based on a profile averaged over a specific width ($w$), exposure of the filter layer can occur locally (*e.g.* in a single profile) while exposure of the filter layer cannot be detected from the averaged profile if besides this local erosion no or less erosion takes place. Therefore, analysis of erosion based on an averaged profile can lead to (hidden) erosion that is not sufficiently accounted for by the damage parameter based on an averaged profile. A damage parameter like $E_{3D}$ is not based on an averaged profile and does not have this disadvantage. However, not using any averaging may cause that variations of the bed not linked to erosion of stones, have a large impact on the damage parameter. To avoid such somewhat misleading characterization of damage, averaging the damage over a circular area of 3 or 5 stone diameters ($E_{3D,3}$ or $E_{3D,5}$) provides a better characterization of the damage than $E_{3D,1}$. As $E_{3D}$ is a maximum value, its value tends to increase when larger section widths, or characterization widths, are considered (de Almeida et al., 2019). This length effect also occurs in real structures (Van Gent et al., 2019).

For above mentioned reasons, $E_{3D,3}$ and $E_{3D,5}$ are considered to be the most suitable damage parameters for mild slopes and are used in the analysis of the test results.

## 3. Physical model tests

### 3.1. Test set-up

The physical model tests (1:6, 1:8 and 1:10 rock-armoured slopes with an impermeable core) have been performed in the Pacific Basin (28 m x 14 m x 1.25 m) at the Deltares in Delft. An impression of the test set-up is presented in Fig. 4. In the middle of the wave basin a wave flume section (1 m width) is constructed where the tested structures are located. The wave paddle has no reflection compensation, but to minimize re-reflections from the basin walls, the reflected waves that reach the wave paddle are spread over the 14 m width, while on both sides of the flume wave dampers are present. On one side of the flume a window section was present to observe the wave interaction visually; seaward of the observation window a wave damper was applied as well. The slope consisted of an impermeable core (steel plates), and an armour layer without a filter layer. The structure consists of stones with a diameter of $D_{n50} = 0.0148$ m. Characteristic velocities under breaking waves acting on the permeable armour layer can roughly be estimated by $u = \sqrt{(gH_s)}$. For the waves in the test programme the laminar contribution to porous flow resistance is estimated at 1%–5% of the total (using the Forchheimer equation). In reality the turbulence contribution dominates, while scale effects are expected if the laminar contribution is important in the model. Although the laminar contribution is not completely negligible, the contribution is small enough to conclude that the scale effects are expected to be minimal. All tests were performed with a JONSWAP wave spectrum with a peak enhancement factor of 3.3. No wave overtopping occurred during the tests. Fig. 5 shows the dimensions concerning the test set-up. The main characteristics of the model are shown in Table 4.

#### 3.1.1. Wave gauges to determine the wave characteristics

The wave characteristics were measured in front of the flume by means of three wave gauges (Fig. 5). The measured signals by these wave gauges have been used to separate the incoming and reflected waves (Zelt and Skjelbreia, 1992).

#### 3.1.2. Camera to determine the type of wave breaking

A camera was used as a measuring tool to determine the distribution between spilling and plunging breaking waves. The position of the camera was above the top of the slope pointing towards the incoming breaking waves. This location is shown on the right side of Fig. 5.

#### 3.1.3. Coloured strips to analyse the eroded and deposited stones

Stones were coloured in strips of 0.5 m. A camera was positioned directly above the flume at a height of approximately 15 m. Photos were taken from a fixed position before and after a test. This made it possible to compare the initial and the damaged slopes. Another camera was positioned underwater at the side of the glass walled section of the flume. This provided indications whether stones were starting to move (rocking, displacements, *etc*).

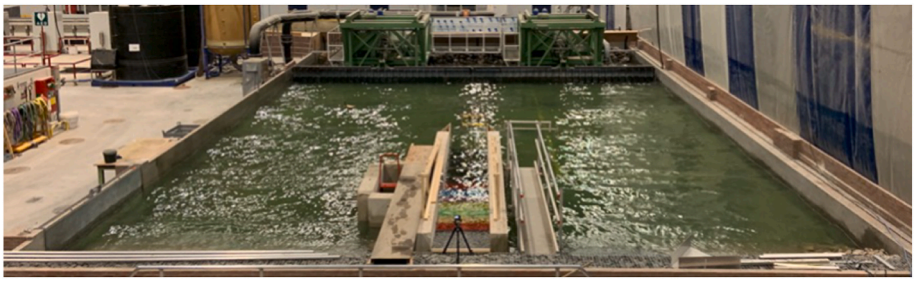

**Fig. 4.** Test section in flume in the middle of the wave basin.

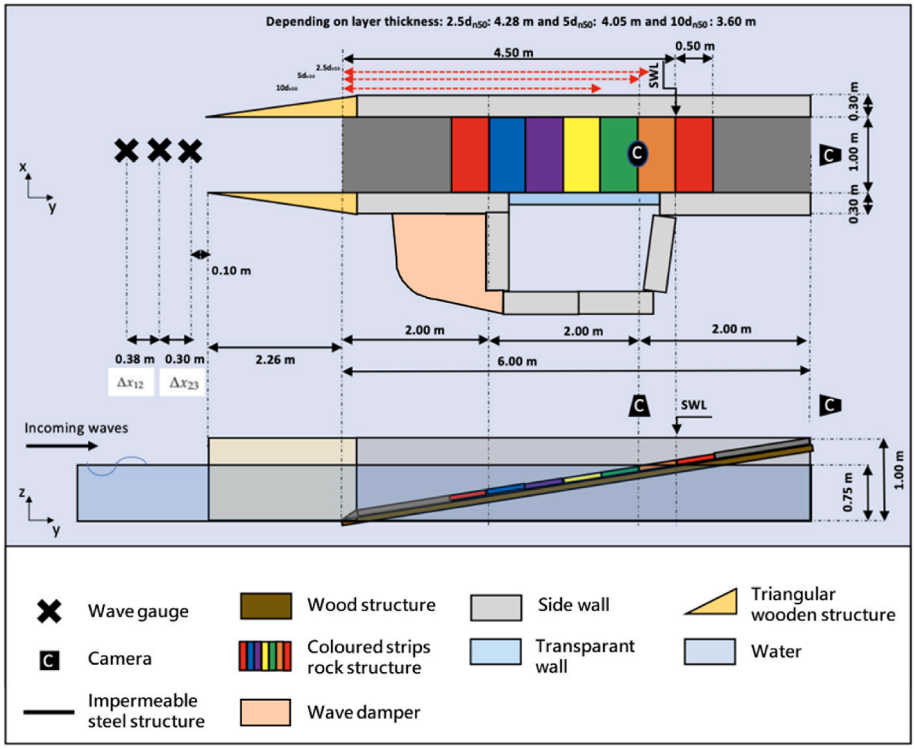


**Fig. 5.** Sketch of test set-up of the flume (1:6).

**Table 4**
Parameter ranges of the test programme.

| Parameter | Symbol | Values/Ranges |
|---|---|---|
| Seaward slope (−) | cot $\alpha$ | 6, 8 and 10 |
| Stone diameter armour layer (m) | $D_{n50}$ | 0.0148 |
| Layer thickness armour layer (m) | $t_a$ | 0.037 (2.5 $D_{n50}$), 0.074 (5 $D_{n50}$) and 0.148 (10 $D_{n50}$) |
| Grading width of armour layer (−) | $D_{85}/D_{15}$ | 1.4 |
| Specific weight of stones (kg/m$^3$) | $P_s$ | 2 944 |
| Relative density of stones (−) | $\Delta$ | 1.94 |
| Water depth (m) | $h$ | 0.75 |
| Incident significant wave height at toe (m) | $H_{m0}$ | 0.02–0.23 |
| Spectral mean wave period (s) | $T_{m\text{-}1,0}$ | 0.6–2.6 |
| Peak wave period (s) | $T_p$ | 0.7–3.0 |
| Wave steepness: $s_{m\text{-}1,0} = 2\pi H_{m0}/gT^2_{m\text{-}1,0}$ (−) | $s_{m\text{-}1,0}$ | 0.009–0.057 |
| Wave steepness: $s_{op} = 2\pi H_{m0}/gT_p^2$ (−) | $s_{op}$ | 0.008–0.052 |
| Surf-similarity parameter: $\xi_{m\text{-}1,0} = \tan\alpha/s^{0.5}_{m\text{-}1,0}$ (−) | $\xi_{m\text{-}1,0}$ | 0.42–1.66 |
| Surf-similarity parameter: $\xi_p = \tan\alpha/s^{0.5}_{op}$ (−) | $\xi_p$ | 0.45–1.67 |
| Number of waves (−) | $N$ | 250–20 000 |

#### 3.1.4. Stereo photography to determine the profile-based damage parameters

Stereo photography is a non-intrusive measurement technique where two or more photos from different locations are used to retrieve elevations, see also Hofland et al. (2011, 2014). The initial and damaged surface profiles were measured using stereo photography to obtain digital representations of the slopes. Fig. 6 shows the camera positions to obtain the profiles before and after the tests. Ground Control Points (GCPs) were used to identify locations on photos with known XYZ coordinates. The resulting digital representations of the slopes before and after a test are used to determine the profile-based damage parameters (*e.g.* $A_e$). The digital representation of the slope before and after a test is obtained with a series of overlapping pictures (more than 30% overlap) with a minimal resolution of 12 Mpx to 24 Mpx. The measurement accuracy of each measurement point is in the order of 1 mm. However, because the results presented are based on difference plots between the slope before and after a test, the bias in the measured slopes is eliminated, and the obtained accuracy in the difference plots is estimated to be an order of magnitude lower than the 1 mm. If a mechanical profiler with a diameter related to the stone diameter would have been used, this could have affected the obtained erosion area. This means that the obtained damage parameters ($S$, $E_{3D,3}$) can to some extend be affected by the applied measurement method.

### 3.2. Test series

Besides variations in the slope (1:6, 1:8 and 1:10) also the thickness of the armour layer was varied (2.5 and 5 times the stone diameter of the armour layer). Varying the slope angles and wave steepness ($0.009<s_{m\text{-}1,0}<0.057$), lead to variations in the surf-similarity ($0.42<\xi_{m-1,0}<1.66$). Table 5 shows an overview of the performed test series. Per test series of a combination of slope and wave steepness, the wave height was increased in steps. The slopes were repaired after reaching the highest wave height within a test series. More detailed information can be found in the theses of Mossinkoff (2019),

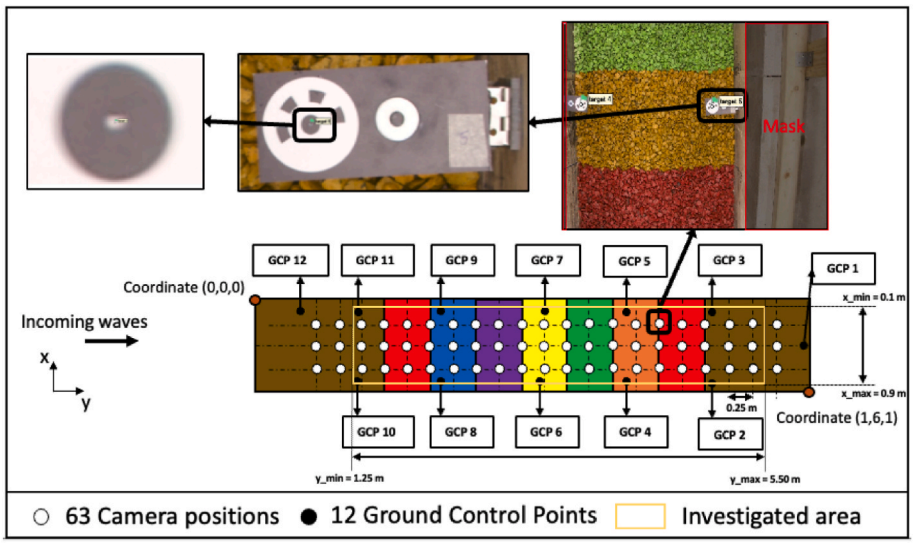


**Fig. 6.** Sketch of the camera positions and the locations of the Ground Control Points including an example of a photo (1:6 slope test).

**Table 5**
Overview of performed test series.

| | Slope | Test series | $s_{m\text{-}1,0}$ | $\xi_{m-1,0}$ | $H_s$ (m) | $N$ | $t_a$ /$D_{n50}$ | Number of tests | Studied parameters |
|---|---|---|---|---|---|---|---|---|---|
| Venrooy (2021) | 1:6 | 1 | 0.012 | 1.46–1.66 | 0.03–0.08 | 1 000 | 2.5 | 8 | $H_s$ and $\xi_{m\text{-}1,0}$ |
| | | 2 | 0.031 | 0.92–1.01 | 0.03–0.12 | 1 000 | 2.5 | 11 | $H_s$ and $\xi_{m\text{-}1,0}$ |
| | | 3 | 0.044 | 0.78–0.87 | 0.04–0.10 | 1 000 | 2.5 | 8 | $H_s$ and $\xi_{m\text{-}1,0}$ |
| | | 4 | 0.047 | 0.76–0.81 | 0.06–0.07 | 250–20000 | 2.5 | 8 | $N$ |
| | | 5 | 0.048 | 0.76–0.77 | 0.08–0.09 | 1 000 | 2.5 | 5 | Variability |
| | | 6 | 0.044 | 0.79–0.83 | 0.04–0.12 | 1 000 | 2.5 | 7 | Variability |
| | | 7 | 0.031 | 0.92–0.97 | 0.05–0.11 | 1 000 | 5 | 10 | $t_a$ |
| | | 8 | 0.013 | 1.47–1.66 | 0.03–0.08 | 1 000 | 5 | 11 | $t_a$ |
| | | 9 | 0.045 | 0.78–0.80 | 0.05–0.16 | 1 000 | 5 | 13 | $t_a$ |
| | | 10 | 0.045 | 0.77–0.82 | 0.04–0.21 | 1 000 | 10 | 14 | $t_a$ |
| Van Wijland (2020) | 1:8 | 1 | 0.012 | 1.11–1.28 | 0.02–0.08 | 1 000 | 2.5 | 8 | $H_s$ and $\xi_{m\text{-}1,0}$ |
| | | 2 | 0.021 | 0.81–0.90 | 0.03–0.11 | 1 000 | 2.5 | 8 | $H_s$ and $\xi_{m\text{-}1,0}$ |
| | | 3 | 0.033 | 0.67–073 | 0.05–0.12 | 1 000 | 2.5 | 14 | $H_s$ and $\xi_{m\text{-}1,0}$ |
| | | 4 | 0.044 | 0.59–0.61 | 0.05–0.17 | 1 000 | 2.5 | 8 | $H_s$ and $\xi_{m\text{-}1,0}$ |
| | | 5 | 0.050 | 0.54–0.57 | 0.06–0.17 | 1 000 | 2.5 | 9 | $H_s$ and $\xi_{m\text{-}1,0}$ |
| | | 6 | 0.034 | 0.67–0.69 | 0.12 | 250–14000 | 2.5 | 8 | $N$ |
| | | 7 | 0.034 | 0.67–0.68 | 0.06–0.16 | 1 000 | 5 | 12 | $t_a$ |
| | | 8 | 0.012 | 1.12–1.23 | 0.03–0.08 | 1 000 | 5 | 11 | $t_a$ |
| | | 9 | 0.035 | 0.66–0.67 | 0.12 | 1 000 | 2.5 | 5 | Variability |
| | | 10 | 0.036 | 0.65 | 0.12 | 1 000 | 2.5 | 1 | Variability and noise of small stones |
| Mossinkoff (2019) | 1:10 | 1 | 0.012 | 0.91–0.94 | 0.06–0.09 | 1 000 | 2.5 | 3 | $H_s$ and $\xi_{m\text{-}1,0}$ |
| | | 11 | 0.012 | 0.91 | 0.07–0.09 | 1 000 | 2.5 | 4 | $H_s$ and $\xi_{m\text{-}1,0}$ |
| | | 2 | 0.035 | 0.52–0.54 | 0.09–0.21 | 1 000 | 2.5 | 8 | $H_s$ and $\xi_{m\text{-}1,0}$ |
| | | 3 | 0.055 | 0.42–0.44 | 0.10–0.20 | 1 000 | 2.5 | 7 | $H_s$ and $\xi_{m\text{-}1,0}$ |
| | | 4 | 0.024 | 0.64–0.67 | 0.08–0.13 | 1 000 | 2.5 | 6 | $H_s$ and $\xi_{m\text{-}1,0}$ |
| | | 5 | 0.045 | 0.46–0.48 | 0.10–0.21 | 1 000 | 2.5 | 7 | $H_s$ and $\xi_{m\text{-}1,0}$ |
| | | 6 | 0.035 | 0.53–0.54 | 0.14–0.15 | 300–11000 | 2.5 | 6 | $N$ |
| | | 7 | 0.013 | 0.87–0.90 | 0.11–0.13 | 1 000 | 5.0 | 3 | $t_a$ |
| | | 8 | 0.036 | 0.53 | 0.16–0.20 | 1 000 | 5.0 | 3 | $t_a$ |

Van Wijland (2020) and Venrooy (2021).

### 3.3. Test results

#### 3.3.1. Spilling waves and plunging waves

Videos of the tests were analyzed to determine the percentage of spilling and plunging waves (no surging waves occur for the tested conditions with mild slopes). Analyzing the breaking type for every single wave is time consuming and therefore only the first 100 waves of each test were used to determine the percentages of spilling and plunging waves. The test condition with the highest significant wave height $H_s$ of each test series is used for the determination of the distribution of spilling and plunging waves. How spilling and plunging waves are distinguished from each other is visualized in Fig. 7. Spilling waves are recognized by a roller starting as indicated in Fig. 7. This roller continues to propagate until the wave run-up zone. A plunging wave is recognized by the curved shape forming a plunging jet. After this plunging jet has reached the slope, a bouncing effect is visible by entrained air and splashing of water.

Fig. 8 shows the percentage of plunging waves (the percentage of spilling waves is 100% minus this percentage) for the three different slopes as function of the surf-similarity parameter or Iribarren number. Fig. 8 indicates that the surf-similarity parameter or Iribarren number is indeed the proper parameter to describe the type of wave breaking (see also Battjes, 1974). For values larger than $\xi_{m-1,0} = 1.0$ about 100% of the waves were plunging waves (test conditions reached values of about $\xi_{m-1,0} = 1.7$). For values smaller than $\xi_{m-1,0} = 1.0$ the fraction of plunging waves $F_P$ (and the fraction of spilling waves is $F_S = 1\text{-}F_P$) can be

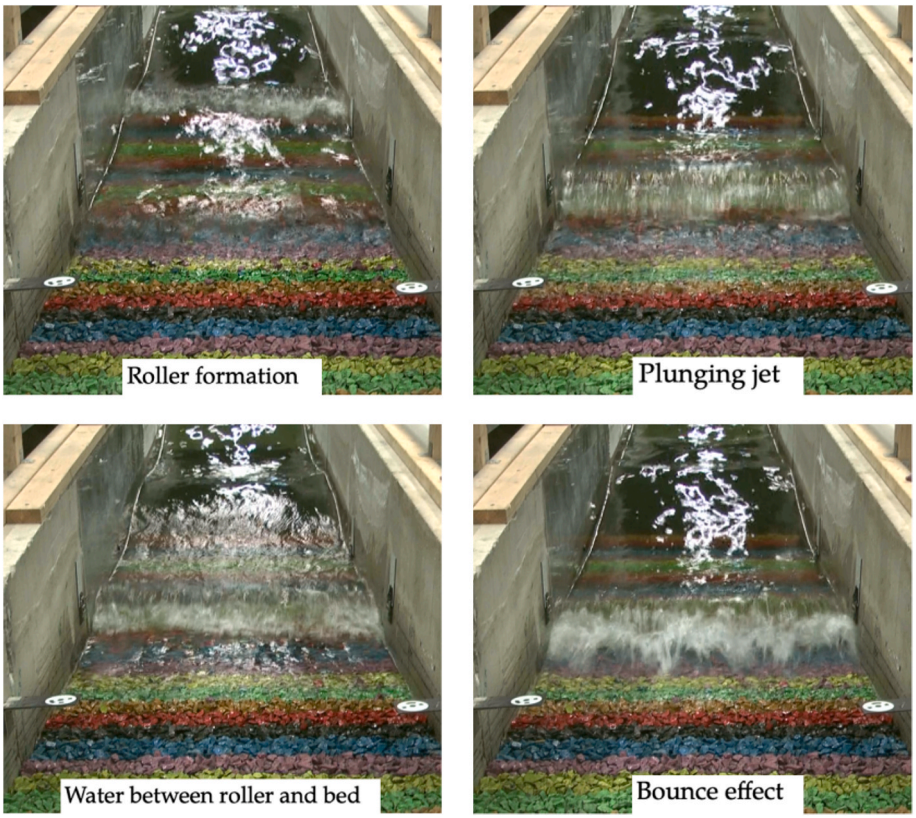


**Fig. 7.** Examples of identification of spilling and plunging breakers. Left column with spilling breaker: the spilling breakers form a small foamy bore that persists over a longer distance on the slope. Right column with plunging breaker: the plunging breaker has a clear overturning crest and has a large splash and bounce-back occurring on a narrower area on the slope.

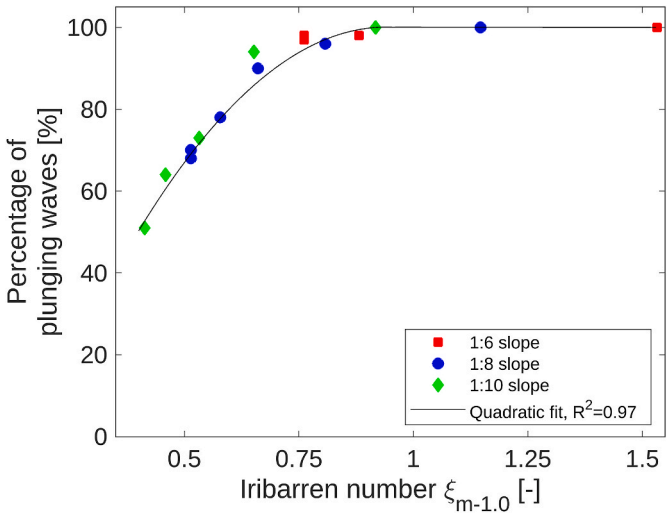


**Fig. 8.** Percentage of plunging waves for slopes 1:6, 1:8 and 1:10 as function of the surf-similarity parameter/Iribarren number (here: percentage of spilling waves is 100% minus percentage of plunging waves).

described by ($R^2 = 0.97$):

$$F_p = \frac{N_{plunging}}{N_{total}} = -1.7\xi_{m-1,0}^2 + 3.2\xi_{m-1,0} - 0.5 \quad \text{for} \quad 0.4 \leq \xi_{m-1,0} \leq 1.0 \tag{6}$$

### 3.3.2. Influence of slope angle

Fig. 9 shows the damage parameters $S$ (left panel) and $E_{3D,3}$ (mid panel) as function of the wave height. For each wave steepness, the damage for 1:6 slopes is systematically larger than the damage for 1:8, while the damage for 1:10 slopes is the lowest for each wave steepness. Thus, in the range of the tested slopes, the damage increases for steeper slopes as expected. The right panel of Fig. 9 shows the relation between the two damage parameters.

A steeper slope, inherent to an increasing surf-similarity parameter, leads to a lower percentage of spilling waves. Another important effect of steeper slopes is the influence of the gravity-component along the slope on the resistance to wave loading and the direction of displaced stones. For a 1:10 slope where the gravity-component along the slope is relatively small, the dominant direction of transport is upward (see also Mossinkoff, 2019). Although, for slope 1:6 the dominant transportation direction is not necessarily downslope for all wave characteristics, especially for the steeper waves on a 1:6 slope, where more downward transportation is observed than for low wave steepness.

Because on mild slopes displaced stones often remain in the region of wave attack, instead of being transported to a much lower position for steeper slopes, it is more likely that displaced stones can eventually end up in an eroded part of the slope, contributing again to the strength of the slope. This also can cause that with a slightly increasing wave height within a test series, sometimes the observed damage can slightly reduce compared to a condition with a slightly lower wave.

### 3.3.3. Influence of wave steepness

Fig. 10 shows for each slope the influence of the wave steepness on the amount of damage. For each slope the conditions with the lowest wave steepness generally lead to the largest damage (for the damage parameter $E_{3D,3}$ there are a few exceptions for a 1:6 slope) and the conditions with the highest wave steepness generally lead to the lowest damage (although there are exceptions, mainly for the damage parameter $E_{3D,3}$). For the steepest slope 1:6 the influence of the wave steepness

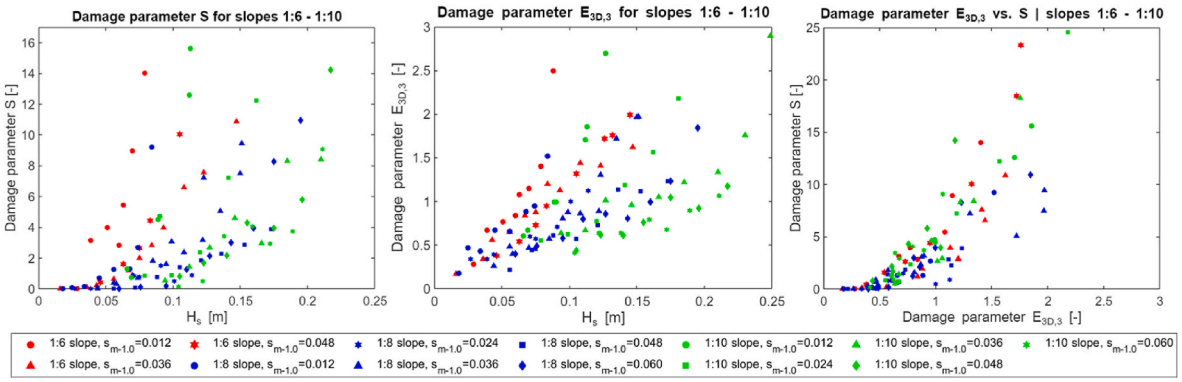


**Fig. 9.** Damage parameters $S$ (left panel) and $E_{3D,3}$ (mid panel) as function of the significant wave height $H_s$ distinguishing between different wave steepness and slope angles (all tests after 1 000 waves with a layer thickness $t_a/D_{n50} = 2.5$), and the relation between damage parameters $S$ and $E_{3D,3}$ (right panel).

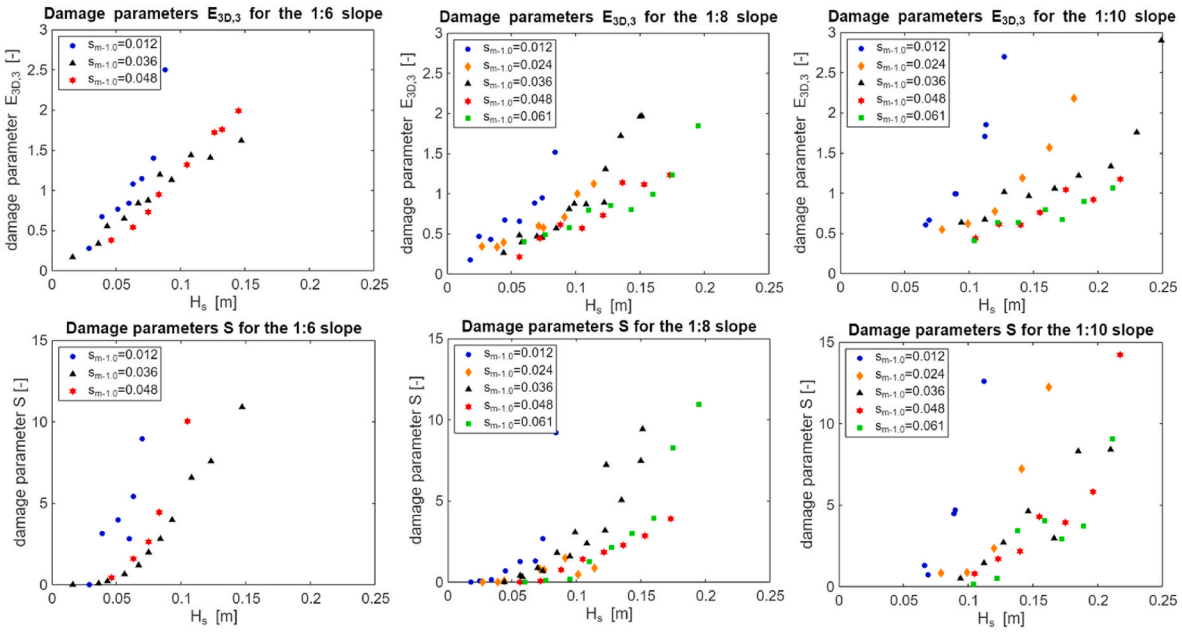


**Fig. 10.** (a) Damage $S$ as function of the significant wave height $H_s$ for varying wave steepness and slopes 1:6, 1:8 and 1:10 with a layer thickness $t_a$ /$D_{n50} = 2.5$ (b) Damage parameter $E_{3D,3}$ compared to significant wave height $H_s$ for varying wave steepness and slopes 1:6, 1:8 and 1:10 with a layer thickness $t_a$ /$D_{n50} = 2.5$.

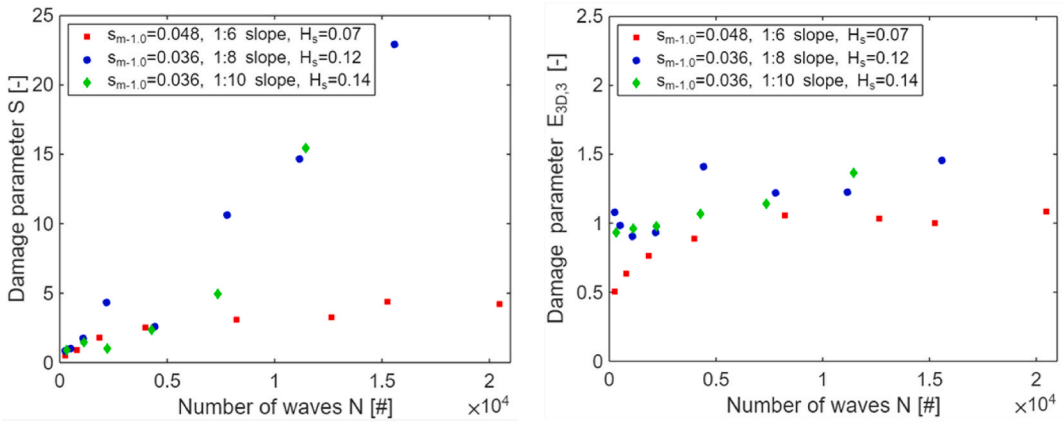


**Fig. 11.** Damage as function of the number of waves $N$ for slopes 1:6, 1:8 and 1:10.

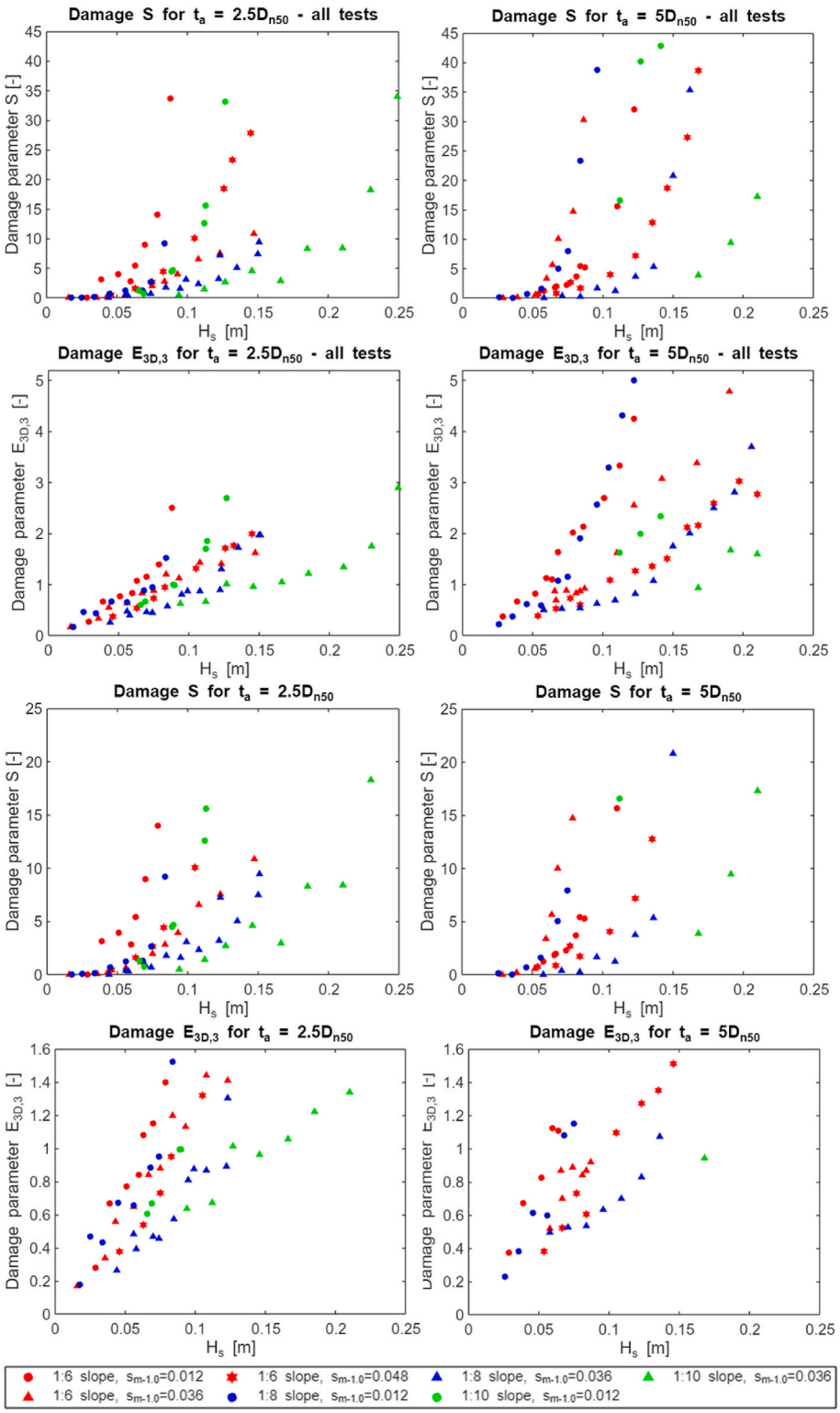


**Fig. 12.** Damage for various armour layer thickness for slopes 1:6, 1:8 and 1:10; left panels for a layer thickness of 2.5 $D_{n50}$, right panels a layer thickness of 5 $D_{n50}$; upper four with all tests, lower four with only the lower ranges of $S$ and for $E_{3D,3} \leq 1.5$.

is much less than for the most gentle slope 1:10. For a specific slope an increased wave steepness leads to a lower value of the surf-similarity parameter or Iribarren number, while a lower value corresponds to a lower percentage of plunging waves. This illustrates that in most cases a lower percentage of plunging waves leads to less damage.

### 3.3.4. *Influence of number of waves*

Fig. 11 shows the damage as function of the number of waves $N$. The damage increases with the number of waves, except for a 1:6 slope where a kind of equilibrium is reached after about 8 000 waves. For slopes 1:8 and 1:10 no equilibrium is reached within the tested range of about 20 000 waves. For the damage parameter $S$ a clear linear upward trend is observed for a 1:8 slope while also an upward trend is present for

a 1:10 slope, although less systematic. For the damage parameter $E_{3D,3}$ no clear linear upward trend is observed. This indicates that with an increasing number of waves the damage spreads over a wider part of the 1:8 and 1:10 slope, but the maximum erosion depth hardly increases for an increasing number of waves.

#### 3.3.5. *Influence of layer thickness*

The tests were performed with an impermeable core. The armour layer was installed on a wooden plate. The thickness of the armour layer has been varied. Fig. 12 shows the damage for different thicknesses of the armour layer (2.5 and 5 times the stone diameter $D_{n50}$). Fig. 12 shows that for the lowest wave steepness and the steepest slope, leading to the highest surf-similarity parameter, there is no clear difference between the damage for the two layer thicknesses (compare red open and filled circles). Also for the highest wave steepness and the most gentle slope, leading to the lowest surf-similarity parameter, there is no clear difference between the damage for the two layer thicknesses (compare green open and filled triangles). However, for some series the tests with the thin armour layer lead to somewhat more damage than thicker armour layer (compare for instance red open and filled stars). It is concluded that the influence of the thickness of the armour layer is more complex than a systematic dependency on the wave steepness, slope and/or surf-similarity parameter. Besides that, damage values depend on the layer thickness, also the criteria for failure depend on the layer thickness, since failure (underlayer visible) occurs much later for thicker armour layers.

## 4. Analysis of test results

### 4.1. *Damage location*

For mild slopes stones move both up and down, and more often than for steep slopes they remain in the wave attack section after displacement. To analyse sections with erosion and accretion use is made of a classification of five damage locations based on Van Wijland (2020), illustrated with an example shown in Fig. 13.

**Low:** Lowest slope location where erosion of an individual stone occurs.

**Mid-Low:** Lowest transect in which erosion of two stones occurs.

**Low-Area:** Lowest transects where stones are displaced over the entire transect.

**Mid-High:** Highest transect in which erosion of two stones occurs.

**High:** Highest slope location where erosion of an individual stone occurs.

All tests with a test duration of 1 000 waves and armour layers with a thickness of 2.5 $D_{n50}$ were used to analyse the location of damage. For each test the damage locations shown in Fig. 13 were determined and the vertical position of these locations were made non-dimensional with the wave height. Per slope the median of damage locations were determined. In Fig. 14 these median values are listed per slope angle, together with the median value of the position of the maximum erosion depth $E_{3D,3}$.

The values shown in Fig. 14 indicate that the upper levels of the affected part (*e.g.* Mid-high: Med MH) are relatively independent on the slope angle while the lower levels of the affected part (*e.g.* Mid-low: Med ML) reach lower levels for the gentler slopes. Thus, the total affected part of the slope becomes wider for gentler slopes, not only because the slope is longer due to the gentler slopes but also due to lower levels that are affected.

Fig. 15 provides an illustration of the variation in the values shown in Fig. 14. The median and the boxplot limits of the upper levels of the affected part of the slope, *i.e.* "Mid-high" and "High", are generally below 0.5$H_s$ and 1$H_s$, respectively. Based on this limited variation, the upper limit of the affected part of the slope can be safely set at SWL+1 $H_s$

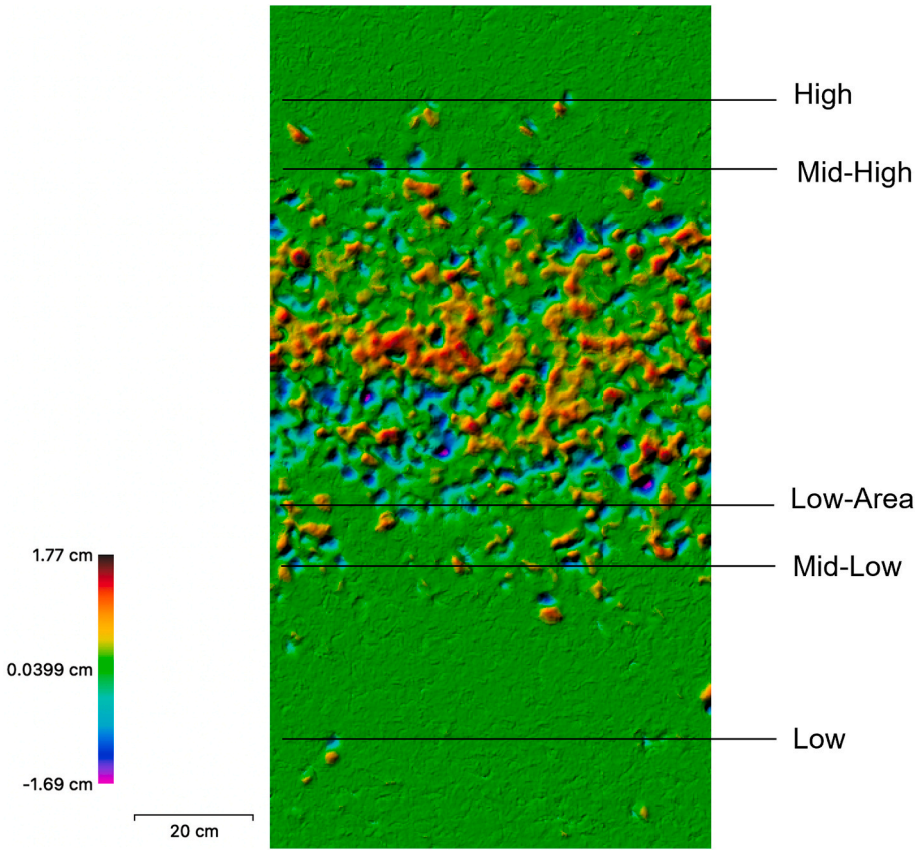


**Fig. 13.** Damage locations (green denotes no displacements, yellow/orange denotes accretion, blue denotes erosion).

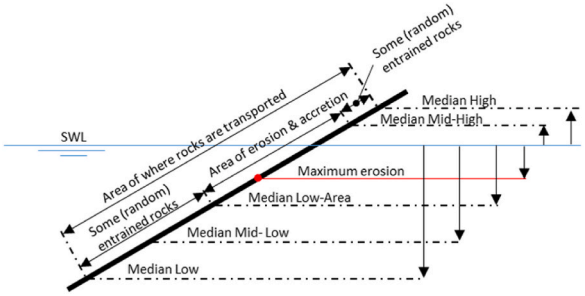


| | 1:6 slope | 1:8 slope | 1:10 slope |
|---|---|---|---|
| Med H | 0.14 | 0.70 | 0.46 |
| Med MH | 0.09 | 0.59 | 0.39 |
| Max $E_{3D,3}$ | -0.25 | -0.41 | -0.76 |
| Med LA | -0.66 | -1.11 | -1.24 |
| Med ML | -1.11 | 1.58 | -1.81 |
| Med L | -1.73 | -2.70 | -2.27 |

**Fig. 14.** Schematization of the damage locations (left) and the corresponding values for each slope are displayed on the right (vertical positions made non-dimensional with $H_s$). The results are based on all tests with a test duration of 1 000 waves and an armour layer thickness of 2.5 $D_{n50}$.

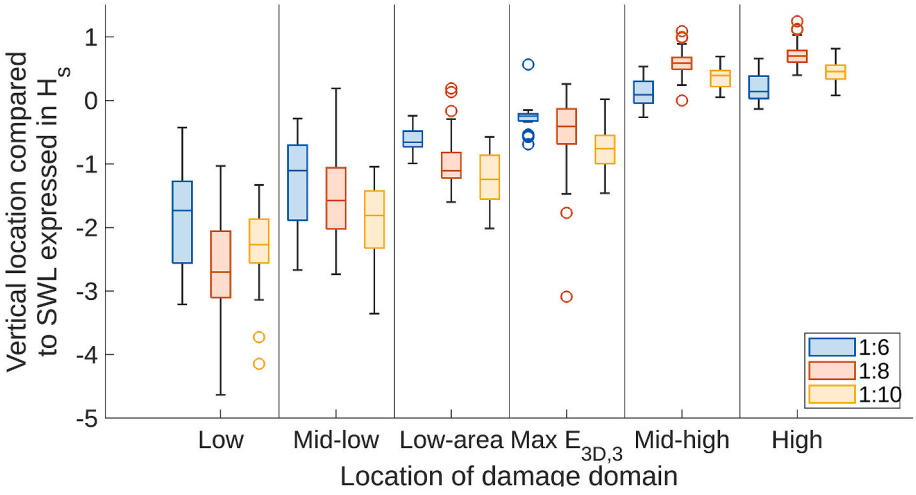


**Fig. 15.** Boxplot of damage domains according to five locations shown in Figs. 13 and 14, for slope 1:6, 1:8 and 1:10.

for all these slopes, using the "Mid-high" level as a characteristic measure. However, for the lower levels of the affected part of the slope, *i.e.* "Mid-low" and "Low" the levels do not only vary per slope but also the variability is larger than for the upper level of the affected slopes. Using the "Mid-low" as a characteristic measure, the lower limit of the affected part of the slope can be safely set at SWL-1.5 H for a 1:6 slope, at SWL-2.0 H for a 1:8 slope, and at SWL-2.5 H for a 1:10 slope.

### 4.2. Damage values

The test results (*e.g.* Figs. 9–11) clearly show that the slope angle, wave steepness, number of waves and layer thickness, all affect the stability of the armour layer on mild slopes. The percentage of spilling and plunging waves can be expressed as a function of the surf-similarity parameter, which consists of a combination of the slope angle and the

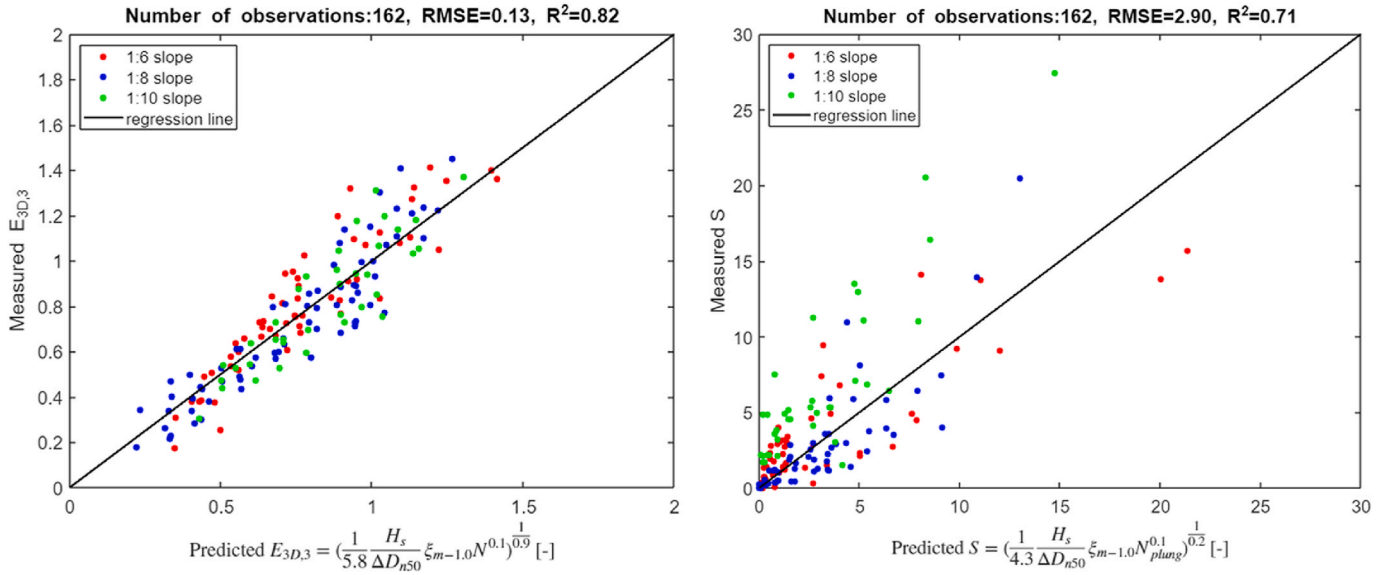


**Fig. 16.** Measured and predicted damage values $E_{3D,3}$ for slopes 1:6 to 1:10.

wave steepness. The fraction of plunging waves depends on the surf-similarity parameter (see Eq. (6)). Thus, to derive an expression that relates the amount of damage ($E_{3D,3}$ is the preferred parameter) to the stability number $H_s/\Delta D_{n50}$, the slope angle, wave steepness and the percentage of plunging waves are the most important to take into account.

Based on the tests for mild slopes in range 1:6 to 1:10 for layer thicknesses $t_a$ in range $2\,D_{n50} \leq t_a \leq 5\,D_{n50}$, an expression describing the test results has been derived for both $E_{3D,3}$ (Eq. (7)) and $S$ (Eq. (8)):

$$\frac{H_s}{\Delta D_{n50}} = \frac{5.8\,E_{3D,3}^{0.9}}{\xi_{m-1,0}\,N_{plunging}^{0.1}} \tag{7}$$

$$\frac{H_s}{\Delta D_{n50}} = \frac{4.3\,S^{0.2}}{\xi_{m-1,0}\,N_{plunging}^{0.1}} \tag{8}$$

where $D_{n50}$ is the stone diameter, $\Delta$ is the relative density of the stones, $E_{3D,3}$ is the maximum erosion depth as defined in Eq. (3), $\xi_{m-1,0}$ is the surf-similarity parameter, and $N_{plunging}$ is the fraction of plunging waves as derived by Eq. (6) and $S$ is the damage parameter. Fig. 16 shows the measured damage versus the computed damage according to Eq. (7) (left) and Eq. (8) (right). The statistical measures RMSE & $R^2$ are also shown in Fig. 16. It can be observed that the RMSE for the fit of $E_{3D,3}$ is significantly lower than for $S$. This suggests that it is better to use $E_{3D,3}$ (Eq. (7)) rather than $S$ (Eq. (8)) for mild slopes.

Note that Eq. (7) and Eq. (8) are considered valid within the tested ranges shown in Table 6. Since all tests were performed with relatively deep water at the toe of the structures, without wave breaking on the foreshore, Eq. (7) can only be used as a preliminary estimate for conditions with important wave breaking on the foreshore. For conditions with severe wave overtopping the expression is likely to give an overestimate since the expression is based on tests without wave overtopping.

### 4.3. Damage criteria

Besides estimating the amount of damage, also criteria on the amount of acceptable damage need to be defined. Use is made of the following damage levels.

- **Start of damage:** a low amount of stones is displaced.
- **Intermediate damage:** displacements of a considerable amount of individual stones but without the filter layer being visible at any position.
- **Failure:** filter layer exposed over an area of at least one squared armour stone diameter.

For in total 45 tests the damage expressed by the damage parameters $S$ and $E_{3D,3}$ are matched to the described damage levels (start of damage, intermediate damage and failure). The values depend on the slope angle, layer thickness and damage parameter ($S$ and $E_{3D,3}$) and are shown in Table 7.

**Table 6**
Ranges of validity of expression (Eq. (7)). *) The tested range is $t_a/D_{n50} = 2.5$–5. The armour layer is allowed to be $t_a = 2\,D_{n50,armour}$ if a filter layer thickness of $t_f \geq 0.5\,D_{n50,armour}$ is used. Corresponding with the structure type with an impermeable core tested in Van der Meer (1988).

| Parameter | Symbol | Values/Ranges |
|---|---|---|
| Stability number (−) | $H_s/\Delta D_{n50}$ | 0.9–7.2 |
| Damage level: maximum erosion depth (−) | $E_{3D,3}$ | 0.3–1.5 |
| Slope (−) | cot $\alpha$ | 6–10 |
| Non-dimensional layer thickness armour layer (−) | $t_a/D_{n50}$ | 2*) - 5 |
| Wave steepness: $s_{m-1,0} = 2\pi H_{m0}/gT_{m-1,0}^2$ (−) | $s_{m-1,0}$ | 0.009–0.057 |
| Surf-similarity parameter: $\xi_{m-1,0} = \tan\alpha/s_{m-1,0}^{0.5}$ (−) | $\xi_{m-1,0}$ | 0.42–1.66 |
| Number of waves (−) | $N$ | 250–20 000 |
| Characterization width | $W/D_{n50}$ | 68 |

**Table 7**
Damage levels based on damage parameters $S$ and $E_{3D,3}$ (*: for these damage levels the criteria could not be determined based on the performed tests, but the $E_{3D,3}$ values for failure are at least larger than 2.5).

| Slope | Damage levels | $t_a = 2$ to 2.5 $D_{n50}$ | | $t_a = 5\,D_{n50}$ | |
|---|---|---|---|---|---|
| | | $S$ | $E_{3D,3}$ | $S$ | $E_{3D,3}$ |
| 1:6 | Start | 2 | 0.8 | 2 | 0.8 |
| | Intermediate | 4 | 1.2 | 7 | 1.5 |
| | Failure | 7 | 1.5 | * | * |
| 1:8 | Start | 3 | 0.8 | 3 | 0.8 |
| | Intermediate | 4 | 1.2 | 7 | 1.5 |
| | Failure | 7 | 1.5 | * | * |
| 1:10 | Start | 4 | 0.8 | 4 | 0.8 |
| | Intermediate | 7 | 1.2 | 10 | 1.5 |
| | Failure | 10 | 1.5 | * | * |

The criteria for damage levels $E_{3D,3}$ for start of damage, intermediate damage, and failure, and the damage levels $S$ are based on the performed tests and the relation between $S$ and $E_{3D,3}$ as indicated in Fig. 9 (right panel). The damage levels for the damage parameter $E_{3D,3}$ are slope independent within the tested range of slopes (1:6–1:10). The damage levels for the damage parameter $S$ appear to be higher for gentler slopes, as also discussed in Section 2.1. Based on extrapolation from $S$-criteria for 1:4 slopes, significantly higher values for failure would be obtained (see also Tables 2 and 3) for 1:8 and 1:10 slopes than those derived from the performed tests (Table 7).

For thick armour layers such as the tested layer with a thickness of 5 stone diameters ($t_a = 5D_{n50}$) failure obviously occurs for higher damage values than those for thinner armour layers. The maximum tested damage number for layer thickness $5D_{n50}$ is $E_{3D,3} = 2.5$. For this value, the filter layer is not yet visible and therefore the damage criteria for failure could not be determined. For a layer thickness $2.5D_{n50}$ the slope fails at a damage value of $E_{3D,3} = 1.5$ or $S = 7$ to 10 (depending on the slope angle).

Besides the explanations described in Section 2.1 this analysis supports the use of $E_{3D,3}$ in a design formula for mildly sloping rock armour layers since the criteria for $E_{3D,3}$ are slope independent, in contrast to the criteria if the damage parameter $S$ is used.

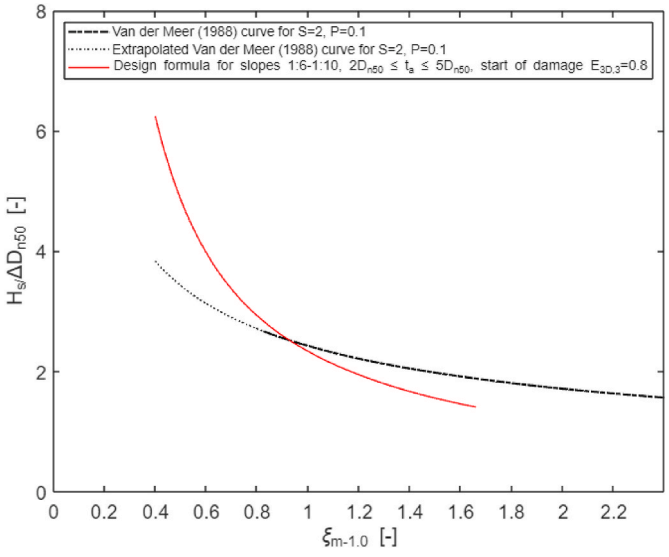


**Fig. 17.** Stability number for start of damage versus the surf-similarity parameter for mild rock-armour slopes (red curve) and for steep slopes according to Van der Meer (1988), both for structures in deep water.

### 4.4. Discussion

As described in Sections 1 and 2, existing expressions to estimate the stability of steep rock-armoured structures cannot accurately be applied for mild slopes. To illustrate this, the stability expression by Van der Meer (1988) for steep rock-armoured slopes in deep water is compared to the expression derived here for mild slopes (Eq. (7)). Fig. 17 shows the derived expression (in green and red) and the expression by Van der Meer (1988), including an extrapolation of the latter. A structure with an impermeable core and damage levels related to "start of damage" using $S = 2$ and $E_{3D,3} = 0.8$, are shown with the stability number on the vertical axis and the surf-similarity parameter on the horizontal axis. This figure clearly shows that for values lower than $\xi_{m\text{-}1,0} = 0.9$ the damage is overestimated if the Van der Meer (1988) is applied. For a value of $\xi_{m\text{-}1,0} = 0.5$ the required $D_{n50}$ is overestimated significantly, which shows that the expression by Van der Meer (1988) should not be applied for mild slopes (1:6 or milder) with wave conditions leading to values lower than $\xi_{m\text{-}1,0} = 0.9$. Note that values lower than $\xi_{m\text{-}1,0} = 0.9$ correspond to conditions for which the contribution of spilling breakers cannot be ignored (see Fig. 8).

Based on the data described in previous sections the expression to estimate the stability of mildly sloping rock armour layers has been derived (Eq. (7)). Table 6 shows the ranges of validity. Although these ranges cover a rather wide range of rock-armoured slopes, there are relevant limitations with respect to the ranges of validity. Although the expressions may be accurate outside the range of the test conditions, the validity is unknown. Some important limitations and other aspects are discussed below.

- **Shallow foreshores**: The derived expression (Eq. (7)) is based on conditions where no significant wave breaking occurs on the foreshore. These types of mild slopes are often in relative shallow water, therefore this limitation can be important. It is not unlikely that for conditions where significant wave breaking occurs before the waves reach the slope, the stability may be different than obtained for the deeper water conditions on which the expression is based (Eq. (7)).
- **Oblique waves**: It is recommended to study the influence of oblique waves on the stability of mild slopes. For oblique wave attack on steep slopes reference is made to Van Gent (2014).
- **Armour layer**: The derived expression is obtained for rock armoured structures with an impermeable core. The effect of an increasing armour layer thickness is tested but no consistent dependency of the stability on the layer thickness has been observed. This requires more detailed research with respect to the layer thickness, including the influence of the layer thickness for thinner armour layers on mild slopes ($t_a < 2D_{n50}$).
- **Slope angle:** The derived expression is obtained based on tests with slopes 1:6, 1:8 and 1:10. Slopes which are milder are not considered in this test programme, but it is likely that the stability becomes higher for slopes milder than 1:10 since the percentage of plunging waves will further decrease, while the affected part of the slope becomes larger. For a 1:10 slope the affected zone is between SWL+1$H_s$ and SWL-2$H_s$. The upper level of the affected zone is constant within the range of tested slopes while the lower level of the affected part reaches lower levels for milder slopes. It is not unlikely that for slopes milder than 1:10, the lower level of the affected part of the slope moves further downward (lower than SWL-2$H_s$).
- **Damage parameters:** The damage of 1:6 slopes is more concentrated in comparison with 1:8 and 1:10 slopes (see also Fig. 14). This indicates that for mild slopes the affected part of the slope increases compared to steeper slopes, leading to a lower erosion depth ($E_{3D,3}$) for the same total eroded area $A_e$ (with $S = A_e / D_{n50}^2$). Thus, for milder slopes a higher allowable $S$ value has been determined. Since the damage criteria for damage parameter $E_{3D,3}$ are slope independent, this indicates that this damage parameter is more suitable to characterize damage than the damage parameter $S$ for which the damage criteria are slope dependent. Also for steep slopes, the damage criteria that indicate failure are slope dependent if the damage parameter $S$ is used. Therefore, the use of the damage parameter $E_{3D,3}$ is also recommended for steeper slopes. The recommended design values for S in Table 7 are lower than those for steeper slopes. This is probably due to the different behaviour of stones on a mild slope. While displaced rocks on steep slopes generally move downward outside the wave attack zone, they move both up and down on a mild slope, and often remain in the wave attack zone. This leads to a lower increase in the averaged damage area $A_e$ ($S = A_e / D_{n50}^2$) for increasing intrinsic damage. For instance, if a rock moves sideways, $A_e$ will remain equal, while a damage hole (increasing $E_{3D}$) appears.
- **Damage criteria:** It is recommended to design for an armour layer for which after wave loading at least one stone diameter of the armour layer remains everywhere. Based on analysis of 28 tests, this corresponds to $E_{3D,3} = 0.8$. This corresponds to the recommendation that thin armour layers ($t_a = 2$ to $2.5D_{n50}$) should be designed for damage values $E_{3D,3}$ corresponding to start-of-damage and not for intermediate damage. For thicker armour layers more damage can be accepted than for thin armour layers, leading to smaller stone diameters for thicker armour layers. For an armour layer thickness of $t_a = 5D_{n50}$, it is recommended to design for an armour layer for which after wave loading at least half of the armour layer remains everywhere. Based on analysis of 7 tests, this corresponds to $E_{3D,3} = 1.5$. This corresponds to the recommendation that thicker armour layers ($t_a \geq 5D_{n50}$) can be designed for damage values $E_{3D,3}$ corresponding to intermediate damage and not for start-of-damage. Above criteria are those related to structures where the material underneath the armour layer is stable (using closed filters or geotextiles). If underneath the armour layer small filter material or sand is applied as an open filter, a thicker armour layer may be required to reduce the wave loading on the interface between the armour layer and underlayer. Since the loading on this interface is affected by damage to the armour layer, criteria for thick armour layers need to be determined in combination with the design of the open filter, see also Van Gent and Wolters (2015, 2018), Van Gent (2016), Jacobsen et al. (2017) and Van Gent et al. (2017).

## 5. Conclusions and recommendations

To estimate the stability of mildly sloping rock-armoured structures, existing guidelines derived for steeper rock-armoured slopes can lead to conservative estimates of the required stone diameter (*e.g.* a factor two larger stone diameters based on extrapolation of existing guidelines). Therefore, physical model tests with mildly sloping rock-armoured structures (*i.e.* 1:6, 1:8 and 1:10) with an impermeable core have been performed. The analysis of tests resulted in the following conclusions.

- Compared to steeper sloping structures, mildly sloping structures lead to a larger fraction of the breaking waves being spilling waves rather than plunging waves. Based on the tests the fraction of spilling and plunging breakers within single wave conditions has been quantified based on the surf-similarity parameter (see also Eq. (6)).
- Compared to steeper sloping structures, mildly sloping structures show a much wider part of the armour layer being affected by erosion and accretion; for mildly sloping structures accretion occurs at lower levels on the slope (reaching lower levels than two significant wave heights below the still water level) than for steeper slopes. Also, stones move both up and down, and more often remain in the wave attack section after displacement.
- Exposure of the layer underneath the armour layer to direct wave attack is generally considered as unacceptable. For mildly sloping rock-armoured structures, the relation between the erosion depth and eroded area of the armour layer is clearly different for mildly sloping structures than for steep rock-armoured structures. For the same local erosion depth much larger values of the eroded area of the

armour layer can be accepted for mildly sloping structures. If damage criteria are based on the eroded area ($S$ or $A_e$) the acceptable amount of damage depends on the slope angle (see also Table 7). By using criteria based on the erosion depth (here preference is given to the damage parameter $E_{3D,3}$), the dependency of the criteria on the slope angle can be avoided. It is recommended to use the damage parameter $E_{3D,3}$ to characterize damage to mild rock-armoured slopes.

- The damage to mildly sloping rock-armoured layers depends on the stability number (*i.e.* wave height, stone diameter and specific weight of the stones), wave steepness, the slope angle, the number of (plunging) waves, and the layer thickness. Within the range of the tested slope angles (*i.e.* 1:6, 1:8 and 1:10), the stability can be estimated based on a newly developed guideline (Eq. (7)). The amount of allowable damage is much larger for thicker armour layers. Based on the analysis, damage criteria have been defined for various layer thickness (Table 7). It is recommended to analyse the influence of the layer thickness into more detail, including layer thicknesses thinner than two stone diameters.

The present tests have been performed for conditions without wave breaking on the foreshore (*i.e.* "deep water" conditions). It is recommended to study the stability of mildly sloping rock-armoured structures also for conditions where wave breaking occurs on the foreshore (*i.e.* "shallow water" conditions), since this could increase the field of application of the presented (or modified if required) guidelines significantly.

The present tests have been performed for structures with an impermeable core. It is recommended to study the stability of mildly sloping rock-armoured structures also for structures with a permeable core.

The present tests indicate that the influence of the thickness of the armour layer is different for mildly sloping rock-armoured structures (*i.e.* no systematic increase in damage for thinner armour layers) than for steep slopes (*i.e.* thicker armour layers are expected to lead to less damage). It is recommended to study the influence of the layer thickness on the amount of expected damage and amount of acceptable damage over a wider range of slope angles and armour layers, than tested in the present test programme.

Although exposure of the layer underneath the armour layer to direct wave attack is considered as unacceptable, the present guidelines for steep rock-armoured structures are often based on the eroded area of the armour layer rather than on the erosion depth. It is recommended to develop also guidelines (estimates of expected damage and criteria of acceptable damage) for steep slopes that are based on the erosion depth rather than on the eroded area of the armour layer.

## CRediT authorship contribution statement

**Daan Jumelet:** Conceptualization, Methodology, Investigation, Formal analysis, Data curation, Visualization, Supervision, Writing – original draft. **Marcel R.A. van Gent:** Conceptualization, Methodology, Investigation, Formal analysis, Data curation, Supervision, Writing – original draft. **Bas Hofland:** Conceptualization, Methodology, Investigation, Formal analysis, Supervision, Review & Editing. **Coen Kuiper:** Conceptualization, Methodology, Investigation, Supervision, Review & Editing.

## Declaration of competing interest

The authors declare that they have no known competing financial interests or personal relationships that could have appeared to influence the work reported in this paper.

## Data availability

Data will be made available on request.

## Acknowledgements

This study was realized with the help of a TKI (Top Consortia for Knowledge and Innovation) subsidy (Delta Technology project Dynamics of Hydraulic Structures) and the support of De Vries & van de Wiel - DEME, Deltares and TU Delft. We acknowledge Lieke Mossinkoff, Bas van Wijland, Tom Venrooy and the staff of the Deltares facilities for setting up and performing the tests.

## References

Allan, J.C., Komar, P.D., 2004. Environmentally compatible cobble berm and artificial dune for shore protection. Shore Beach 1, 1.
Battjes, J.A., 1974. Computation of Set-Up, Longshore Currents, Run-Up and Overtopping Due to Wind-Generated Waves. Ph.D.-thesis (TU Delft).
Bayle, P.M., Blenkinsopp, C.E., Conley, D., Masselink, G., Beuzen, T., Almar, R., 2020. Performance of a Dynamic Cobble Berm Revetment for Coastal Protection, under Increasing Water Level. https://doi.org/10.1016/j.coastaleng.2020.103712.
Bayle, P.M., Kaminsky, G.M., Blenkinsopp, C.E., Weiner, H.M., Cottrell, D., 2021. Behaviour and Performance of a Dynamic Cobble Berm Revetment during a Spring Tidal Cycle in North Cove. Washington State, USA. https://doi.org/10.1016/j.coastaleng.2021.103898.
Broderick, L.L., 1983. Riprap stability, a progress report. Proc. Coastal Structures '83. ASCE 320–330.
Broderick, L.L., 1984. Riprap Stability versus Monochromatic and Irregular Waves, PhD Thesis. Oregon State University.
de Almeida, E., Van Gent, M.R.A., Hofland, B., 2019. Damage characterization of rock slopes. Marine Science and Engineering 60 (7). https://doi.org/10.3390/jmse7010010.
Etemad-Shahidi, A., Bali, M., van Gent, M.R.A., 2020. On the stability of rock armored rubble mound structures. Coast. Eng. 158 https://doi.org/10.1016/j.coastaleng.2020.103655.
Herrera, M., Gomez-Martin, E., Medina, J.R., 2017. Hydraulic stability of rock armors in breaking wave conditions. Coast. Eng. 127, 55–67.
Hofland, B., Van Gent, M., Raaijmakers, T., Liefhebber, F., 2011. Damage evolution using the damage depth. Proc. Coastal Structures. https://doi.org/10.1142/9789814412216_0070, 2011.
Hofland, B., Disco, M., Van Gent, M.R.A., 2014. Damage characterization of rubble mound roundheads. Proc. Coastlab, 2014.
Hudson, R.Y., 1959. Laboratory investigation of rubble-mound structures, ASCE Transactions. J. Waterw. Harb. Div. 271, 610–659.
Jacobsen, N.G., van Gent, M.R.A., Fredsoe, J., 2017. Numerical modelling of the erosion and deposition of sand inside a filter layer. Coast. Eng. 120, 47–63. Elsevier.
Loman, G.J.A., van Gent, M.R.A., Markvoort, J.W., 2010. Physical Model Testing of an Innovative Cobble Shore; Part 1: Verification of Crossshore Profile Deformation. Proc. Coastlab 2010, Barcelona.
Melby, J., Kobayashi, N., 1998. Progression and variability of damage on rubble mound breakwaters, ASCE. J. Waterw. Port, Coast. Ocean Eng. 124, 286–294.
Mossinkoff, L., 2019. Stability of Stones on Mild Slopes under Wave Attack. Delft University of Technology. M.Sc. thesis. http://resolver.tudelft.nl/uuid:37a20ee8-8bd6-456f-9148-f7520895b908.
Rock Manual, 2007. The Use of Rock in Hydraulic Engineering. CIRIA, second ed. CIRIA, CUR, CETMEF, London. Published by C683, ISBN 978-0-86017-683-1 and 5.
Schiereck, G.J., Fontijn, H.L., Grote, W.V., Sistermans, P.G.J., 1994. Stability of rock on beaches. Proc. ICCE 1994, ASCE 1, 1553–1567. https://icce-ojs-tamu.tdl.org/icce/article/view/5056/4734.
Schiereck, G.J., Fontijn, H.L., 1996. Pipeline protection in the surf zone. Proc. ICCE 1996, ASCE 1, 4228–4241. https://doi.org/10.9753/icce.v25.%25p.
Sistermans, P.G.J., 1993. Stability of Rock on Beaches. Delft University of Technology. M.Sc. thesis. http://resolver.tudelft.nl/uuid:522d417a-63b9-4889-8c7e-813c8d07400e.
Thompson, D., Shuttler, M., 1975. Riprap Design for Wind Wave Attack, a Laboratory Study in Random Waves.
Van der Meer, J.W., 1988. Rock slopes and gravel beaches under wave attack. In: PhD Thesis. Delft University of Technology, Delft, The Netherlands.
Van der Meer, J.W., 2021. Rock armour slope stability under wave attack; the van der Meer formula revisited. Journal of coastal and hydraulic structures 1, 8, 2021.
Van Wijland, J.F.S., 2020. Stability of Rock on Mild Slopes. Delft University of Technology. M.Sc. thesis. http://resolver.tudelft.nl/uuid:b1438a6d-6814-49a1-8798-4082ac01da16.
Van Gent, M.R.A., Smale, A., Kuiper, C., 2003. Stability of Rock Slopes with Shallow Foreshores, Coastal Structures Conference 2003 (Portland).
Van Gent, M.R.A., 2010. Dynamic Cobble Beaches as Sea Defence. Proc. Coastlab 2010, Barcelona.
Van Gent, M.R.A., 2014. Oblique wave attack on rubble mound breakwaters. Coast. Eng. 88, 43–54. https://doi.org/10.1016/j.coastaleng.2014.02.002. Elsevier.

Van Gent, M.R.A., Wolters, G., 2015. Granular slopes with open filters under wave loading. Coast. Eng. 104, 135–150. https://doi.org/10.1016/j.coastaleng.2015.06.004.
Van Gent, M.R.A., 2016. Coastal Structures with Open Filters under Wave Loading, Keynote at Coastlab 2016. Proc. Coastlab 2016, Ottawa.
Van Gent, M.R.A., Jacobsen, N.G., Wolters, G., 2017. Modelling of open filters under wave loading. Proc. ICE Breakwaters 2017, Liverpool. https://doi.org/10.1680/cmsb.63174.1081.
Van Gent, M.R.A., Wolters, G., 2018. Effects of storm duration and oblique wave attack on open filters underneath rock armoured slopes. Coast. Eng. 135, 55–65. https://doi.org/10.1016/j.coastaleng.2018.01.009. Elsevier.
Van Gent, M.R.A., de Almeida, E., Hofland, B., 2019. Statistical analysis of the stability of rock slopes. J. Mar. Sci. Eng. 7 (60) https://doi.org/10.3390/jmse7030060, 2019.
Venrooy, T., 2021. Stability of Stones on Mild Slopes. Delft University of Technology. M.Sc. thesis. http://resolver.tudelft.nl/uuid:4506317c-cf42-4450-bad3-580223b4c546.
Wit, E.M., 2015. Stability of Gravel on Mild Slopes in Breaking Waves. Delft University of Technology. M.Sc. thesis. http://resolver.tudelft.nl/uuid:de18c232-1f82-4101-88a8-62515a3a31b1.
Ye, L., 1996. Stability of Rock on Beaches. Delft University of Technology. M.Sc. thesis. http://resolver.tudelft.nl/uuid:597b65b3-6e4d-495a-b86e-81213a439e61.
Zelt, J.A., Skjelbreia, J.E., 1992. Estimating incident waves and reflected wave fields using an arbitrary number of wave gauges. SAVE Proc. https://doi.org/10.9753/icce.v23.%25p. ICCE 1992, Venice.